

TITANIUM OXIDE NANOTUBE ARRAYS USED IN IMPLANT MATERIALS

Sami A. AJEEL¹, Abdulkareem M. ALI², Zamen KARM³

Electrochemical self-ordering has been recognized as one of the most attractive synthetic approaches for fabrication of highly ordered nanotube materials from a variety of metals and semiconductors. This work presents synthesis of the self-organized TiO₂ nanotube arrays by electrochemical anodization in fluoride/glycerol electrolyte. Scanning electron microscopy and X-ray diffraction were carried out to characterize the well-ordered titanium oxide nanotubes. The corrosion of pure titanium and anodized titanium were tested in synthetic body plasma solution at 37±1°C, using potentiodynamic polarization. It was shown that anodized titanium exhibits superior corrosion resistance compared to pure titanium.

Keywords: titanium oxide nanotube arrays, implants, corrosion, potentiodynamic polarization

1.Introduction

Titanium and its alloys are widely used in biomedical field for hard tissue replacements because of their desirable properties, such as relatively low elastic modulus, good fatigue strength, formability, and corrosion resistance. However, titanium and its alloys are still not sufficient for long-term clinical usage because the biocompatibility and bioactivity of these materials must be improved. Titanium and its alloys are bio inert metallic materials and they cannot bond to living bone directly at the early stage after implantation into a human body. Their surfaces play an important role in the response of the artificial devices in a biological environment and in order of titanium and its alloys to meet the clinical demands it is necessary to modify the surface of the titanium materials. Different surface modifications have been developed to improve the biocompatibility, bioactivity, osteoconductivity, and osseointegration of titanium implants [1]. The different research groups obtained TiO₂ nanotube films with several geometry and characteristics of the surface [2,3]. According to the electrochemical conditions, the high-aspect ratio and self-organized TiO₂ films can be developed during titanium anodized [4-6]. The mechanism of the titanium nanotube formation

¹ Department of Production Engineering & Metallurgy, University of Technology, Iraq, e-mail: engm614@yahoo.com

² Department of Chemistry, University of Baghdad, Iraq

³ Department of Production Engineering & Metallurgy, University of Technology, Iraq

during anodized was studied and discussed in many works before and it is finally considered that the main processes that take place within the electrolyte during anodized was explained [7-9]. The two physical characteristics which determine implant corrosion are thermodynamic forces which cause corrosion either by oxidation or reduction reaction and the kinetic barrier such as surface oxide layer which physically prevents corrosion reactions [10-12]. The synthesis of the nanostructured materials is one of the challenges among nanotechnologies. The applications of these nanomaterials cover a large spectrum, especially in bioscience: drug delivery, nanomedicine, cell growth, or optical properties [13,14].

In the present investigation, development and surface modification of titanium by anodizing techniques to enhance implant integration are studied together with the effects of some process parameters of anodizing titanium. Corrosion behavior of pure titanium and titanium oxide nanotubes in synthetic blood plasma solution is also investigated.

2. Experimental

2.1 Preparation of titanium oxide nanotubes

In this work, a common two-electrode electrochemical cell was used with the working electrode titanium foil (0.25 mm thickness, 99.01% purity) and the counter electrode platinum foil (0.25 mm thickness, 99.7%). Anodization was carried out in 100 mL glycerol with the addition of 5 wt% NH_4F at 10 V and 30V for 10 min. The titanium specimens before anodized can be stress relieved without adversely affecting strength or ductility. Stress-relieving treatments decrease the undesirable residual stresses that result from non uniform hot forging or deformation from cold forming and straightening. The stress relief was done at 500°C for 1/2 h in order to reduce residual stresses developed during fabrication and used protective furnace atmosphere by nitrogen gas [15]. Field emission scanning electron microscope (Hitachi FE-SEM model S-4160, Japan) was utilized for morphological and structural characterization. X-ray diffraction analysis (XRD, using Rigaku D/Max-2200/PC, $\text{CuK}\alpha$ equipment) was performed for crystal phase identification.

2.2 Electrochemical measurements

Potentiodynamic polarization were carried out in synthetic body plasma solution; the chemical composition of solution is given in Table 1. The experiments were performed at pH 7.4 and $37 \pm 1^\circ\text{C}$ temperature, 10 min. for pure titanium and anodized titanium [16].

Corrosion tests were performed using a potentiostat (type Mlab 2000, Germany). All potentials were measured with respect to a saturated calomel electrode (SCE, 200 mV vs. NHE at $37 \pm 1^\circ\text{C}$) as the reference electrode and a platinum rod was used as counter electrode for current measurement. For the potentiodynamic polarization experiment, the test was conducted at a scanning rate of 2 mVs^{-1} . From the obtained polarization curves, the corrosion current density (I_{corr}) was determined by Tafel extrapolation with the aid of a commercial software (Power CORR, V.2.42).

Table 1

Chemical composition of synthetic body plasma solution

Synthetic Blood Plasma		
No.	Constituent	Concentration (g/L)
1	NaCl	6.800
2	KCl	0.400
3	CaCl ₂	0.200
4	NaHCO ₃	2.200
5	Na ₂ HPO ₄	0.126
6	NaH ₂ PO ₄	0.026
7	MgSO ₄	0.100

3. Results and discussion

3. 1. Anodized titanium

Electrochemical anodization was performed in 100 mL glycerol with the addition of 5 wt% NH₄F at 10 V and 30V for 10 min. The appearance of the anodic oxides on the titanium foils is dependent on the applied potential in the electrolyte contained fluoride. An increase in cell voltage from 10 to 30 V results in increasing average pore diameter from 50 nm to 64 nm as indicated by SEM micrographs. Fig. 1 shows that typical surface morphology and cross-section of titanium oxide nanotubes are formed at anodized potential of 10 V. The average pore size is 50 nm with an average tubes length of 1.05 μm .

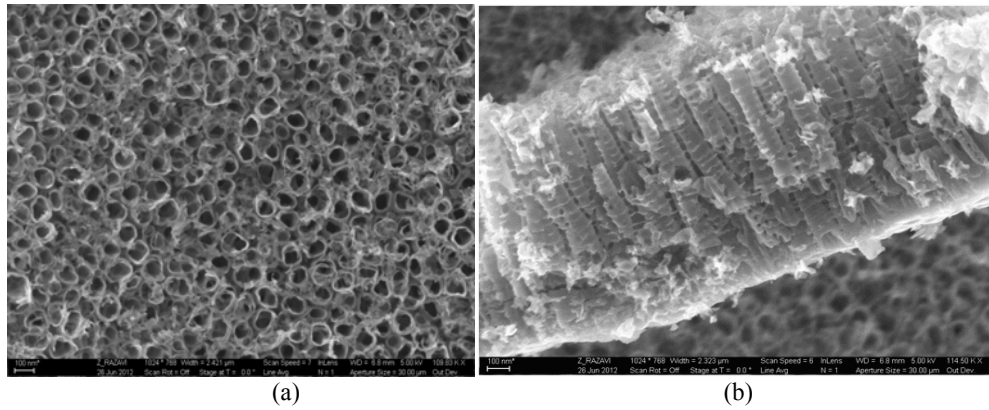


Fig. 1. SEM image of anodized titanium nanotubes at 10V .
(a) top-view (b) cross-section.

Fig. 2 shows that typical surface morphology and cross-section of titanium oxide nanotubes are formed at anodized potential of 30 V. The average pore size is 64 nm with an average tubes length of 1.17 μm .

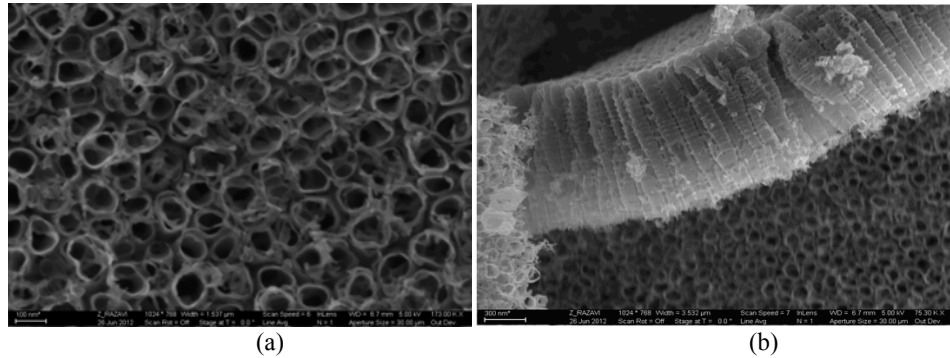


Fig. 2. SEM image of anodized titanium nanotubes at 30V. (a) top-view; (b) cross-section

Figs. 3 and 4 show the results of x-ray diffraction test which was carried out on the specimens of anodized titanium to determine the existing phases in each specimen.

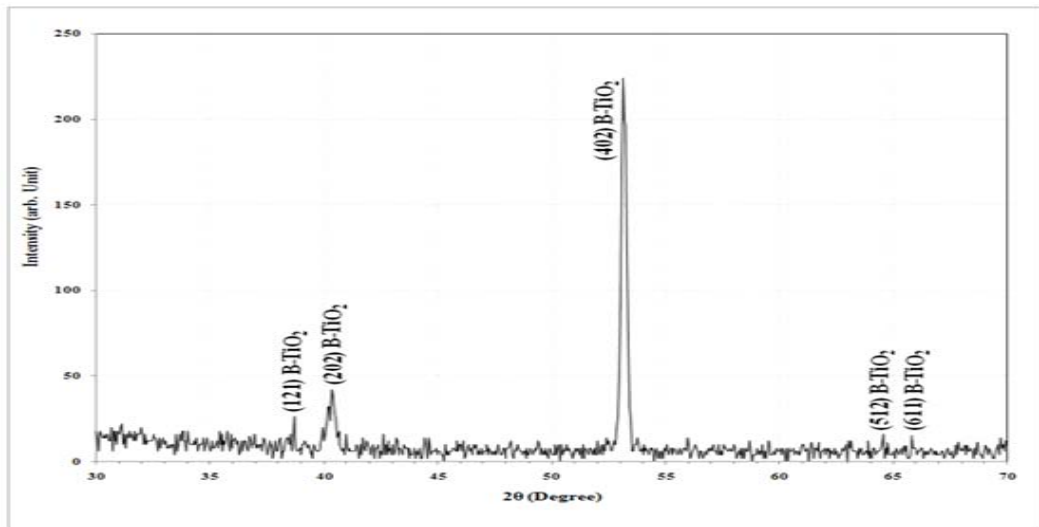


Fig. 3. X-ray diffraction pattern of TiO_2 nanotubes prepared at 10 V

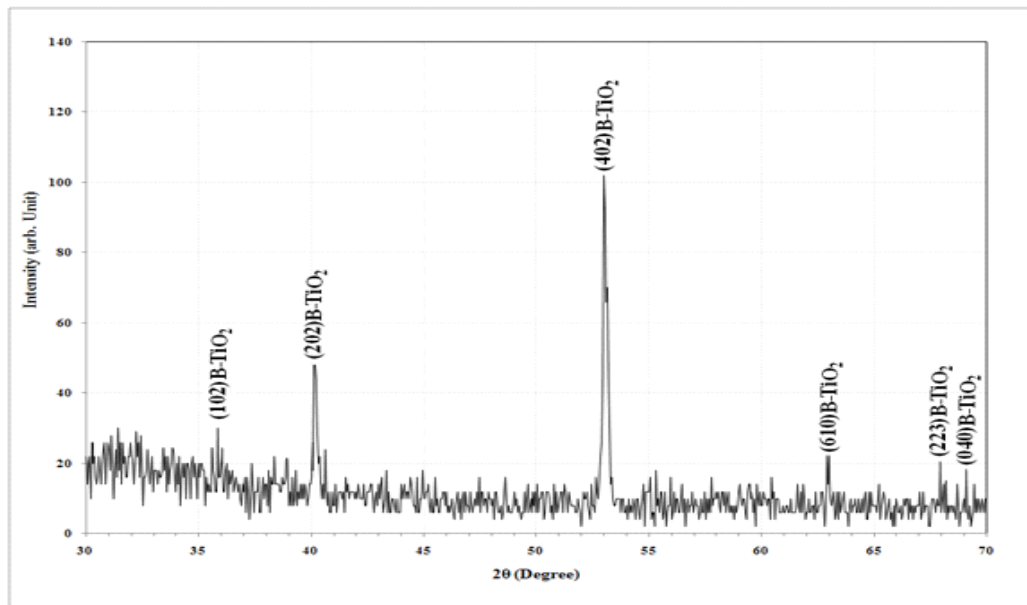


Fig. 4. X-ray diffraction pattern of TiO_2 nanotubes prepared at 30 V

The range of the diffraction angle (2θ) was 30° – 70° . The phases of anodized titanium were determined by calculating d – spacing (using Bragg's

law) compared with standard x-ray diffraction of the (ASTM) standards cards taken from Match Program version 1.9b (2012). X-ray diffraction showed that the titanium oxide nanotube arrays have brookite (amorphous) structures for all anodized specimens. Tables 2 and 3 indicate the obtained values of the following parameters: d-spacing, intensity, phases, and Miller indices (hkl).

Table 2

XRD results for titanium oxide nanotubes prepared at 10 V

$2\theta_{Exp.}$ [degree]	d_{Exp} [Å]	Intensity (arb. unit)	d_{Std} [Å]	hkl	Phase	Card No.
38.69	2.3276	20	2.3346	(121)	Brookite	96-900-9088
40.18	2.2446	32	2.2487	(202)	Brookite	96-900-9088
53.04	1.7267	224	1.7155	(402)	Brookite	96-900-9088
64.66	1.4416	7	1.4436	(512)	Brookite	96-900-9088
65.91	1.4172	8	1.4181	(611)	Brookite	96-900-9088

Table 3

XRD results for Titanium oxide nanotubes prepared at 30 V

$2\theta_{Exp.}$ [Degree]	$d_{Exp.}$ [Å]	Intensity (arb. unit)	$d_{Std.}$ [Å]	hkl	Phase	Card No.
36.12	2.4871	12	2.4827	(102)	Brookite	96-900-9088
40.18	2.2441	48	2.2487	(202)	Brookite	96-900-9088
53.01	1.7276	102	1.7155	(402)	Brookite	96-900-9088
62.92	1.4772	16	1.4749	(610)	Brookite	96-900-9088
67.88	1.3809	13	1.3870	(223)	Brookite	96-900-9088
69.05	1.3603	16	1.3657	(040)	Brookite	96-900-9088

3.2. Potentiodynamic polarization measurements

This study was done to avoid damage of the tissue and to create a good biocompatibility of the prostheses. We needed for this purpose to predict with tests and models the consequences of the implantation surgery. For the tests and models all biological, biomedical and mechanical parameters consulted from literature were used [17]. Polarization curve is commonly used as a plot of the electrode potential versus the logarithm of current density. The potentiodynamic

polarization curves for pure titanium and titanium oxide nanotubes specimens are presented in Figs. 5-7 which show cathodic and anodic branches of polarization curves of pure titanium and anodized titanium specimens in synthetic body solutions. These figures indicate that corrosion potentials of anodized specimens are more noble than that non-anodized specimen.

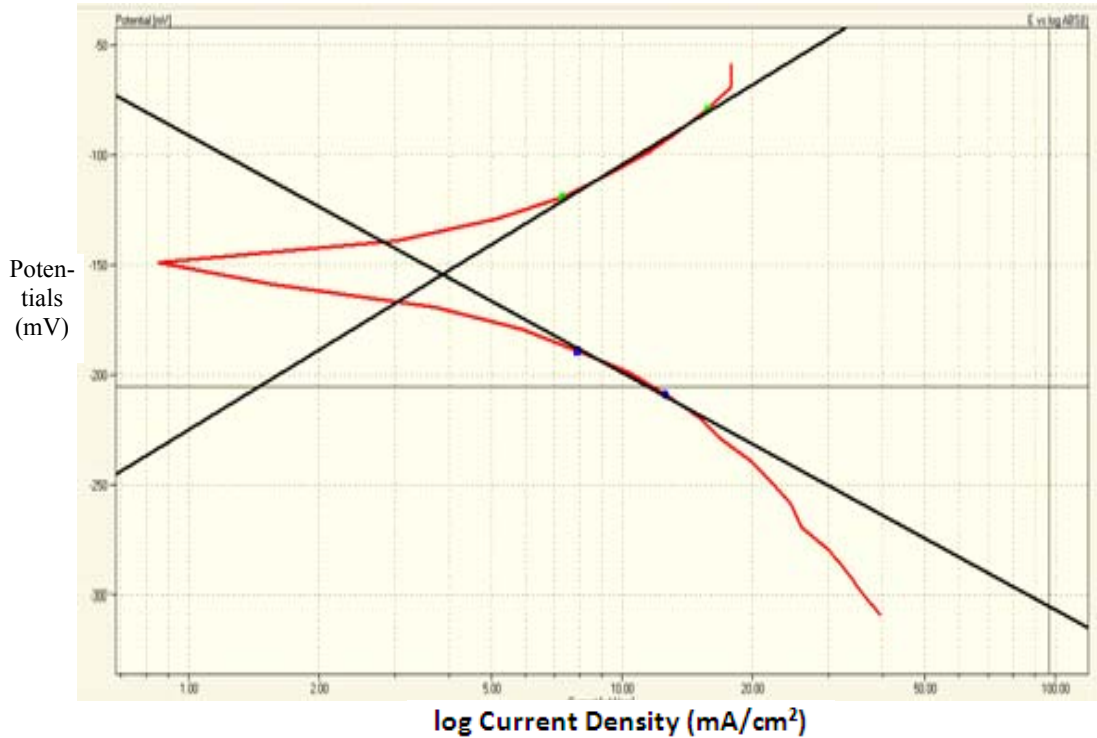


Fig. 5. Potentiodynamic polarization behavior of pure titanium in synthetic blood plasma solution

Fig. 5 indicates such curve in synthetic plasma blood solution, for pure titanium without anodized; it shows that corrosion potential (E_{corr}) and corrosion current density (I_{corr}) values are -150 mV and $4.32 \mu\text{Acm}^{-2}$, respectively. Fig. 6 illustrates the case of anodized titanium at 10 V.

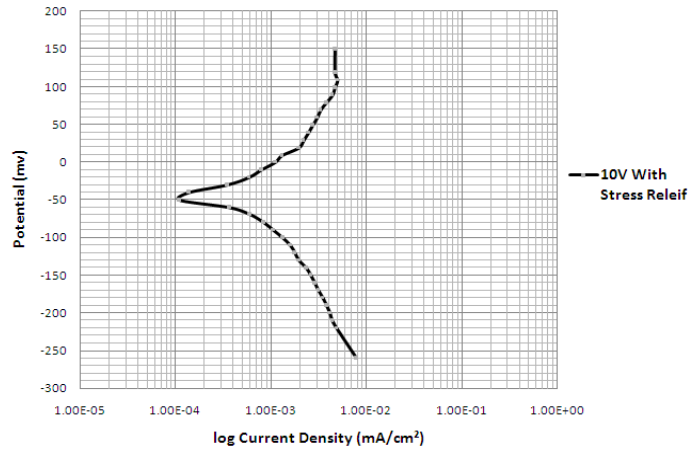


Fig. 6. Potentiodynamic polarization behavior in synthetic blood plasma for anodized titanium at 10 V

It shows that corrosion potential (E_{corr}) and corrosion current density (I_{corr}) values for anodized titanium at 10 V are -50 mV and $1.2 \mu\text{Acm}^{-2}$. The results demonstrate an obvious protection to the metal due to the anodized layer that covers the metal surface.

Fig. 7 presents E-log I curve for anodized titanium at 30 V.

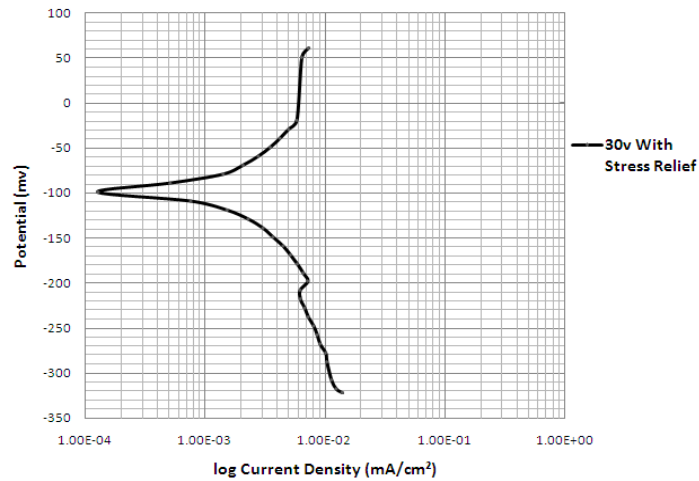


Fig. 7. Potentiodynamic polarization behavior in synthetic blood plasma for anodized titanium at 30 V

This shows that corrosion potential (E_{corr}) and corrosion current density (I_{corr}) values for anodized titanium at 30 V are -110 mV and $1.95 \mu\text{Acm}^{-2}$, respectively.

The results indicate that the anodizing titanium at 30 V has the largest corrosion current density. This may be explained by the large pores leading to a dissolution faster than for the surface of anodizing titanium at 10V.

For comparison of corrosion behavior of titanium and anodized titanium in synthetic body solutions at $37 \pm 1^\circ\text{C}$, Table 4 also illustrates the values of corrosion rate expressed in milli-inches per year (mpy) that can be obtained by using its usual equation [18].

Table 4

Corrosion parameters of specimens in synthetic blood plasma solution				
No	State	E_{corr} (mV)	I_{cor} (μAcm^{-2})	Corros.rate (mpy)
1	Pure titanium	-150	4.32	$5.1 \cdot 10^{-6}$
2	Titanium anodized at 10 V	-50	1.21	$1.7 \cdot 10^{-6}$
3	Titanium anodized at 30 V	-110	1.95	$2.61 \cdot 10^{-6}$

6. Conclusions

From the results obtained by testing samples of pure titanium and titanium oxide nanotubes, it can be concluded that the anodization of titanium specimens for the same time of processing in glycerol with the addition of 5 wt% NH_4F depends on the value of working voltage. Increasing of the applied voltage increases the pores diameter of titanium oxide nanotubes. All TiO_2 nanotubes layers synthesized in this work have a brookite phase structure. Corrosion current density of pure titanium in synthetic blood plasma solution is higher than that of anodized titanium.

REFERENCES

- [1]. X. Liu, K. Paul *et al.*, Surface modification of titanium, titanium alloys, and related materials for biomedical applications, in Mater. Sci. Eng., **vol. 47**, 2004, pp. 49-121
- [2]. G. Andrei, T. Hiroaki *et al.*, Titanium oxide nanotubes prepared in phosphate electrolytes, in Electrochem. Commun., **vol. 7**, 2005, pp. 505–509
- [3]. C. Manole, C. Pirvu *et al.*, Evaluation of TiO_2 nanotubes changes after ultrasonication treatment, in Molec. Cryst. Liq. Cryst., **vol. 521**, 2010, pp. 84-92
- [4]. Q. Rafael, A model for the self structuring of nanotubes in titanium oxide, in Trans.Nanotechnol., **vol. 7**, No. 3, 2008, pp. 371 – 375
- [5]. M. Jan, T. Hiroaki *et al.*, High-aspect ratio TiO_2 nanotubes by anodization of titanium, in Angew. Chem. Int. Ed. Engl, **vol. 44**, 2005, pp. 2100 –2102

- [6]. X. Peng, B. Betzaida *et al.*, TiO₂ nanotube arrays fabricated by anodization in different electrolytes for biosensing, in *Electrochem. Commun.*, **vol. 9**, 2007, pp. 2441–2447
- [7]. P. Madhav, I.P. Song *et al.*, Influence of heat treatment on morphological changes of nano-structured titanium oxide formed by anodic oxidation of titanium in acidic fluoride solution, in *Bio-Medical Mater. Eng.*, **vol. 19**, 2009, pp. 77–83
- [8]. E. Feschet-Chassot, V. Raspal *et al.*, Tunable functionality and toxicity studies of titanium dioxide nanotube layers, in *Nanotechnol.*, 2010, pp. 1-10
- [9]. C. Manole, C. Pirvu, Surface and electrochemical analysis for the understanding of TiO₂ nanopores/nanotubes changes in post-elaboration treatment, in *Surf. Interf. Anal.*, **vol. 521**, 2010, pp. 11-23
- [10]. J.J. Joshua, J.L. Gilbert, R.M. Urban, Current concepts review corrosion of metal orthopaedic implants, in *J. Bone Joint Surg.*, **vol. 80**, 1998, pp. 268-282
- [11]. J.R. Atkinson, B. Jobbins, Properties of engineering materials for use in body, in: D. Dowson, V. Wright Eds., *Introduction to biomechanics of joint and joint replacement*, Mech. Eng. Publ., London, 1981, pp. 141-145
- [12]. P.K. Chu, J.Y. Chen, L.P. Wang, N. Huang, Plasma-surface modification of biomaterials, in *Mater. Sci. Eng. Rep.*, **vol. 36**, 2002, pp. 143-206
- [13]. S. Sathish, V. Anbarasan *et al.*, Corrosion resistance of laser nitrided Ti-13Nb-13Zr titanium and Ti-13Nb-13Zr biomedical alloys, in *Trans. Indian Inst. Met.*, **vol. 61**, 2008, pp. 235-238
- [14]. C. Ravariu, E. Manea *et al.*, Titanium dioxide nanotubes on silicon water designated for Gox enzymes immobilization, *Digest J. Nanomater. Biostruct.*, **vol. 6**, No. 2, 2011, pp. 703-707
- [15]. J. Williams, E. Starke *et al.*, The role of thermomechanical processing in tailoring the properties of aluminum and titanium alloys, in G. Krauss, Ed., *Deformation, Processing, and Structure*, American Society for Metals, New York, pp.1-2173, 1984
- [16]. C. Sella, J. Martin *et al.*, Biocompatibility and corrosion resistance in biological media of hard ceramic coatings sputter deposited on metal implants, *Mater. Sci. Eng.*, **vol. 13**, 1991, pp. 49-57
- [17]. S.Y. Kwon, T. Lin, H. Takei, Q. Ma, D.J. Wood, D. O'Connor, K.L.P. Sung, Alterations in the adhesion behavior of osteoblasts by titanium particle loading: Inhibition of cell function and gene expression, in *Biorheology*, **vol. 38**, 2001, pp. 161–183
- [18]. A. Sami, I. Jamal *et al.*, Improvement of corrosion resistance for carbon steel alloy (ST-52) used in marine environment, *Eng. Technol.*, **vol. 3**, 2005, pp. 1-6